

# Slow Evaporation of Water from Hydrated Salen Transition Metal Complexes in the Gas Phase Reveals Details of Metal Ligand Interactions

Sang-Won Lee, Sukbok Chang,<sup>†</sup> Dmitri Kossakovski, Heather Cox, and J. L. Beauchamp\*

Contribution from the Beckman Institute, California Institute of Technology, Pasadena, California 91125

Received May 18, 1999

**Abstract:** Water clusters of salen [*N,N'*-ethylenebis(salicylideneaminato)] transition metal complexes [(salen)M, M = Cr<sup>3+</sup>, Mn<sup>3+</sup>, Co<sup>3+</sup>] formed by electrospray source have been investigated using a Fourier transform ion cyclotron resonance (FT-ICR) mass spectrometer. Kinetics of water evaporation from the cluster ions is observed to be highly dependent on the central metal ion. For example, the evaporation rate of water from solvated salen chromium ion ([SCr + *n*H<sub>2</sub>O]<sup>+</sup>) is significantly slower than that from solvated salen manganese ([SMn + *n*H<sub>2</sub>O]<sup>+</sup>) and solvated salen cobalt ([SCo + *n*H<sub>2</sub>O]<sup>+</sup>) ions. Furthermore, the clusters of salen chromium ions with two waters attached exhibit special stability, indicated by their prominence in the overall cluster distribution. In contrast, no specific solvation is observed for the manganese and cobalt complexes. The lability observed for the hydrated salen cobalt complex suggests that the high-spin state is likely to be involved in the evaporation process. These results are in accordance with observations in solution-phase chemistry and can be explained by ligand field theory.

## Introduction

Studies of water clusters of ionic species in the gas phase have been providing basic insights into the chemical reactivity and dynamics of ions in the condensed phase. Extensive studies of hydrated metal ions in the gas phase using various experimental techniques have provided a wealth of information on interaction between singly charged metal ions and small ligands such as water.<sup>1</sup> A few experiments on water clusters of multiply charged metal ions have been reported.<sup>2,3</sup> Studies of multiply charged ions are often complicated by reactions in which charge is transferred from the metal ion to solvent molecules (Coulomb explosion). However, the introduction of electrospray ionization<sup>4</sup> has facilitated the production of solvated peptides<sup>5</sup> and organic compounds<sup>6</sup> as well as that of solvated multiply charged metal ions. Recently Posey and co-workers demonstrated that the

clusters of tris(2,2'-bipyridyl)iron(II) complex with a variety of solvents are possible to generate by resolving the electrospray-generated organometallic compound with solvent vapor.<sup>7</sup>

A detailed understanding of the interaction of organometallic complexes with solvent molecules is of interest in the fields of chemistry and biology. Metal ions in the forms of organometallic complexes of many biological systems such as metalloenzymes are essential to their catalytic function and structural stability.<sup>8</sup> In the present study we investigate water clusters of salen transition-metal complexes (structure **1**) generated by an electrospray source. Early interest in these organometallic compounds was driven from their catalytic ability of oxygen or nitrogen transfer.<sup>9</sup> Salen transition-metal complexes have also been investigated as model systems for biologically important processes, such as photosynthetic oxidation of water within photosystem II, and their working structures have been precisely characterized by X-ray crystallographic studies.<sup>10</sup> X-ray data show that two water molecules coordinate to the central metal ions to form an octahedral complex in hydrated crystals.

In this paper, we investigate the slow evaporation of water from hydrated salen transition-metal (**1**, M = Cr<sup>3+</sup>, Mn<sup>3+</sup>, Co<sup>3+</sup>) complexes in the gas phase using FT-ICR. FT-ICR,<sup>11</sup> with its capabilities of ultrahigh mass resolution, mass selection, and

\* To whom correspondence should be addressed.

<sup>†</sup> Present address: Department of Chemistry, Ehwa Womans University, Seoul, Korea.

(1) (a) Kebarle, P. *Annu. Rev. Phys. Chem.* **1977**, *28*, 445. (b) Keesele, R. G.; Castleman, A. W. *J. Phys. Chem. Ref. Data* **1986**, *15*, 1011. (c) Marinelli, P. J.; Squires, R. R. *J. Am. Chem. Soc.* **1989**, *111*, 4101. (d) Dalleska, N. F.; Honma, K.; Sunderlin, L. S.; Armentrout, P. B. *J. Am. Chem. Soc.* **1994**, *116*, 3519. (e) Beyer, M.; Berg, C.; Görlitzer, H. W.; Schindler, T.; Achatz, U.; Albert, G.; Niedner-Schatteburg, G.; Bondybej, V. E. *J. Am. Chem. Soc.* **1996**, *118*, 7386.

(2) (a) Blade, A. T.; Jayaweera, P.; Ikonoum, M. G.; Kebarle, P. J. *J. Chem. Phys.* **1990**, *92*, 5900. (b) Rodriguez-Cruz, S. E.; Jockusch, R. A.; Williams, E. R. *J. Am. Chem. Soc.* **1998**, *120*, 5842. (c) Peschke, M.; Blades, A. T.; Kebarle, P. J. *Phys. Chem. A* **1998**, *102*, 9978.

(3) Stace, A. J.; Walker, N. R.; Firth, S. *J. Am. Chem. Soc.* **1997**, *119*, 10239.

(4) (a) Yamashita, M.; Fenn, J. B. *J. Phys. Chem.* **1984**, *88*, 4451. (b) Fenn, J. B.; Mann, M.; Meng, C. K.; Wong, S. F.; Whitehouse, C. M. *Science* **1989**, *246*, 64.

(5) (a) McLuckey, S. A.; Glish, G. L.; Asano, K. G.; Bartmess, J. E. *Int. J. Mass Spectrom. Ion Processes* **1991**, *109*, 171. (b) Chowdhury, S. K.; Chait, B. T. *Anal. Chem.* **1991**, *63*, 1660. (c) Chowdhury, S. K.; Katta, V.; Chait, B. T. *Rapid Commun. Mass Spectrom.* **1990**, *4*, 81. (d) Rodriguez-Cruz, S. E.; Klassen, J. S.; Williams, E. R. *J. Am. Soc. Mass Spectrom.* **1997**, *8*, 565.

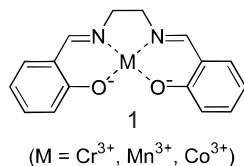
(6) Nguyen, V. Q.; Chen, X. G.; Yergey, A. L. *J. Am. Soc. Mass Spectrom.* **1997**, *8*, 1175.

(7) Spence, T. G.; Burns, T. D.; Posey, L. A. *J. Phys. Chem. A* **1997**, *101*, 139.

(8) Glusker, J. P. In *Advances in Protein Chemistry*; Anfinsen, C. B., Edsall, J. T., Eisenberg, D. S., Richards, F. M., Eds.; Academic: San Diego, CA, 1991; Vol. 42.

(9) Jacobsen, E. N. In *Comprehensive Organometallic Chemistry II*; Wilkinson, G., Stone, F. G. A., Abel, E. W., Hegedus, L. S., Eds.; Pergamon: New York, 1995; Vol. 12, Chapter 11.1.

(10) (a) Aurangzeb, N.; Hulme, C. E.; McAuliffe, C. A.; Pritchard, R. G.; Watkinson, M.; Bermejo, M. R.; Garcia-Deibe, A.; Rey, M.; Sanmartin, J.; Sousa, A. *J. Chem. Soc., Chem. Commun.* **1994**, 1153. (b) Limburg, J.; Vrettos, J. S.; Liable-Sands, L. M.; Rheingold, A. L.; Crabtree, R. H.; Brudvig, G. W. *Science* **1999**, *283*, 1524.



long ion storage times, is ideally suited for studies of the properties, structures, and reaction dynamics of large ions and ionic clusters in the gas phase. We have recently developed a methodology to generate and investigate water clusters of ionic species of interest with employment of "soft" ion sampling conditions in an electrospray source.<sup>12</sup> In these experiments, clusters with special stability are identified as prominent features (magic numbers) in the overall cluster distribution during the evaporation process. In the present study we observe that the kinetics of water evaporation from solvated salen complexes is highly dependent on the central metal ion. Our results are in accord with observations in solution-phase chemistry and can be explained by ligand field theory. Studies of solvated salen transition-metal complexes in the gas phase provide a unique opportunity to investigate transition-metal–ligand interactions without the complications introduced by the presence of counterions.

## Experimental Section

**Instrumentation.** All experiments were performed in an external ion source 7T FT-ICR mass spectrometer that has been described in detail elsewhere.<sup>13</sup> Briefly, the instrument is equipped with a rf-only octopole ion guide to transfer the ions from the atmospheric pressure ion source into the ICR cell. An electromechanical shutter is located between the ESI source and the octopole to maintain pressures below 10<sup>-9</sup> Torr at the ICR cell. The shutter was opened for 2 s to allow ions continuously being generated by the ESI source to enter the octopole ion guide. The rf-field of the octopole was turned on only during this period of time. Argon collision gas (~3 ms pulse, 10<sup>-6</sup> Torr) was introduced to moderate the kinetic energy of the ions while they were travelling through the octopole ion guide and being trapped in the ICR cell. For production of hydrated salen transition-metal complexes a modified version of a commercially available electrospray ion source (Analytica of Branford, Branford, CT) was used that has been described elsewhere.<sup>13</sup> Loss of water from highly solvated ions in a vacuum results in significant evaporative cooling. For example, protonated water clusters are cooled to temperature in the range of 130–150 K.<sup>12,14</sup> The temperature is determined by the balance between evaporative cooling and energy input due to background blackbody infrared radiation and varies over a wide range between water loss events.<sup>15</sup> As the desolvation process nears completion (after 30 s of ion storage in the present study), however, the clusters approach ambient temperature, assumed to be the cell temperature, 295 K. With the time scales of evaporation processes for the systems presented in this work, the cluster temperature may equilibrate with the ambient temperature, but we have no means of ascertaining this possibility.<sup>16</sup> In extracting the experimental rate constants from the variation of ion abundances with time there was no indication that the rates were changing with time for the mono- and dihydrates, which might result from a temporal variation in the cluster

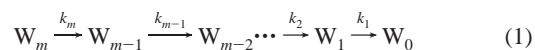
temperatures. For the present study, temperature is measured by a thermocouple located just outside the ICR cell. The probe has been calibrated against another thermocouple that was temporarily installed inside the ICR cell. The salen complexes were dissolved in pure deionized water containing 0.01% acetic acid at concentrations around 50 μM.

**Synthesis of (Salen)Mn<sup>III</sup>Cl.** To a solution of *N,N*-bis(salicylidene)ethylenediamine (1.34 g, 5.00 mmol) in ethanol (20 mL) was added solid Mn<sup>III</sup>(OAc)<sub>3</sub> (as a dihydrate, 1.47 g, 5.48 mmol) and the reaction mixture was refluxed for 2 h under an atmosphere of nitrogen. After the mixture was cooled to room temperature, LiCl (0.25 g, 5.90 mmol) was added as a solid and then the reaction mixture was stirred for additional 1 h at the reflux temperature under air. Brown precipitate formed upon cooling the reaction mixture. The solid was filtered and washed with water (50 mL) and then ether (20 mL). Recrystallization from ethanol gave the brownish product (1.37 g, 88%).

**Synthesis of (Salen)Cr<sup>III</sup>Cl.** To a solution of *N,N*-bis(salicylidene)ethylenediamine (1.07 g, 4.00 mmol) in THF (20 mL) was added CrCl<sub>2</sub> (0.54 g, 4.40 mmol) as a solid and the reaction mixture was refluxed for 2 h under an atmosphere of N<sub>2</sub>. After the mixture was cooled to room temperature, LiCl (0.20 g, 4.72 mmol) was added as a solid and then the reaction mixture was refluxed for additional 1 h under air. After this mixture was cooled to room temperature, a brownish solid was filtered and washed with water (30 mL) and then ether (20 mL). Successive recrystallization from ethanol and from acetone gave the product (0.92 g, 66%).

**Synthesis of (Salen)Co<sup>III</sup>Cl.** To a solution of *N,N*-bis(salicylidene)ethylenediamine (1.0 g, 3.7 mmol) in THF (45 mL) was added cobalt(II) acetate tetrahydrate (1.0 g, 4.0 mmol) as a solid at room temperature. The solution turned a dark brown color immediately. After the mixture was stirred for 2 h at room temperature under N<sub>2</sub> atmosphere, a solution of I<sub>2</sub> (0.51 g, 2.01 mmol) in methylene chloride (10 mL) was added and stirring was continued for an additional 1 h at room temperature. The solvent was evaporated under reduced pressure and the greenish solid residue was recrystallized from ethanol and subsequently from acetone to afford the product (1.2 g, 72%).

**Simulation of Solvent Evaporation Kinetics.** Typical experiments include taking mass spectra of water clusters at different detection delays. Water evaporates from the clusters to eventually yield naked ions at sufficiently long times. As in previous studies from our laboratory,<sup>12</sup> water evaporation was observed to occur by sequential loss of single water molecules:



For the consecutive elementary reaction, the concentration of a specific cluster,  $W_i$ , with  $i$  water molecules, at given time  $t$  is given by:

$$W_i(t) = \sum_{n=0}^{m-i} C_{i+n}^i W_{i+n}^0 e^{-k_{i+n}t} \quad (2)$$

where  $W_i$  and  $W_i^0$  are concentrations of the  $i$ th cluster at time  $t$  and 0,  $m$  is the largest cluster size at  $t = 0$ , and  $k_i$  is the evaporation rate constant of the  $i$ th cluster. By solving ordinary first-order differential equations, the coefficients,  $C$ , are defined iteratively by:

$$C_{i+n}^i = \frac{k_{i+1}}{k_i - k_{i+n}} C_{i+n}^{i+1} \quad (\text{for } n = 1, \dots, m-i) \quad (3)$$

$$C_i^i = 1 - \frac{\sum_{n=1}^{m-i} C_{i+n}^i W_{i+n}^0}{W_i^0} \quad (4)$$

(16) To more completely model the kinetics of evaporation reactions we have initiated a collaborative effort with Professor John Klassen at the University of Alberta. In this experiment we will measure binding energies of water-to-salen transition-metal complexes using high-pressure mass spectrometry.

(11) Marshall, A. G.; Verdun, F. R. In *Fourier Transforms in NMR, Optical, and Mass Spectrometry: A User's Handbook*; Elsevier: Amsterdam, 1990.

(12) Lee, S.-W.; Freivogel, P.; Schindler, T.; Beauchamp, J. L. *J. Am. Chem. Soc.* **1998**, *120*, 11758.

(13) Rodgers, M. T.; Campbell, S.; Marzluff, E. M.; Beauchamp, J. L. *Int. J. Mass Spectrom. Ion Processes* **1994**, *137*, 121.

(14) Schindler, T.; Berg, C.; Niedner-Schatteburg, G.; Bondybey, V. E. *Chem. Phys. Lett.* **1996**, *250*, 310.

(15) For considerations of the relationship between the kinetics of reactions induced by background infrared radiation and energetic parameters such as activation energies, see: Dunbar, R. C.; McMahon, T. B. *Science* **1998**, *279*, 194.

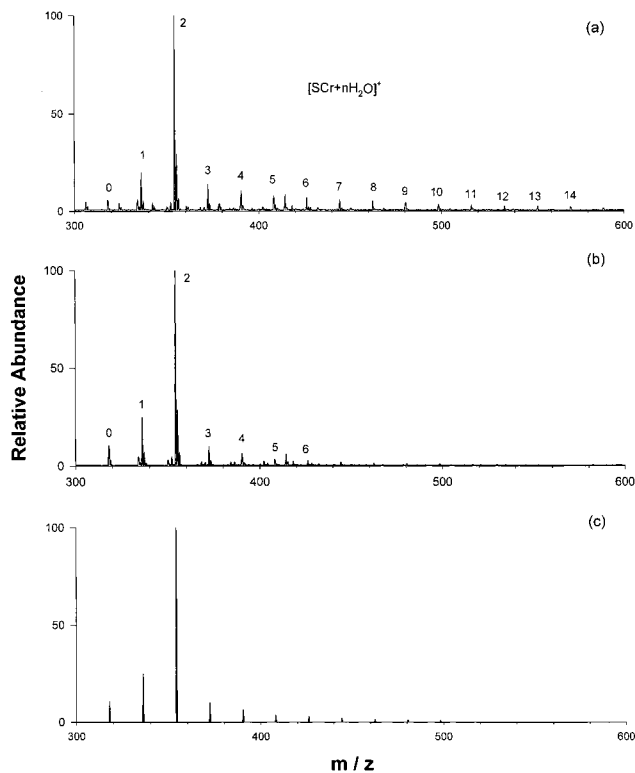


**Figure 1.** An example of the simulation method described in the text: (a) a cluster distribution at 13 s; (b) a cluster distribution at 18 s; and (c) a calculated distribution.

With the temporal variation of concentrations, it is possible to numerically simulate water cluster distributions at various detection times by using the observed  $W_i(t)$  values. An example is shown in Figure 1. Parts a and b in Figure 1 are the two sets of water cluster distributions experimentally measured at 13 and 18 s. Since the distribution at 18 s results from evaporation of water from the distribution observed at 13 s, one can use intensities of water clusters at 13 s as  $W_i^0$  and numerically calculate rate constants that result in relative intensities ( $W_i$ ) of water clusters at 18 s. Figure 1c presents the calculated distribution of water clusters at 18 s, which agrees well with the observed distribution (Figure 1b). A modified simplex method<sup>17</sup> by Nelder and Mead was used for the numerical optimization and the computation is terminated when the  $\chi^2$  value is less than  $1 \times 10^{-8}$ .

## Results and Discussion

**Cluster Distributions of the Salen Complexes with Different Central Metal Ions.** Mass spectra of water clusters of the salen manganese complex taken at various detection delays after ion accumulation are shown in Figure 2. Extensively hydrated salen manganese complexes with as many as 60 water molecules are observed. *No evidence for special stability of the dihydrate complex ion is observed.* Similarly, no specific solvation is observed for water clusters of the salen cobalt complex (Figure 3). This is rather surprising since two water molecules are known to bind directly to central metal ions and presumably have stronger binding energies than the outer shell water ligands. It indicates that the water ligands are labile in these complexes, which will be discussed more in following sections.

With chromium as the central metal ion, however, cluster distributions (Figure 4) clearly indicate that the dihydrate has special stability. The two waters undergo slow evaporation over 100 s, while the larger clusters disappear in 20 s.

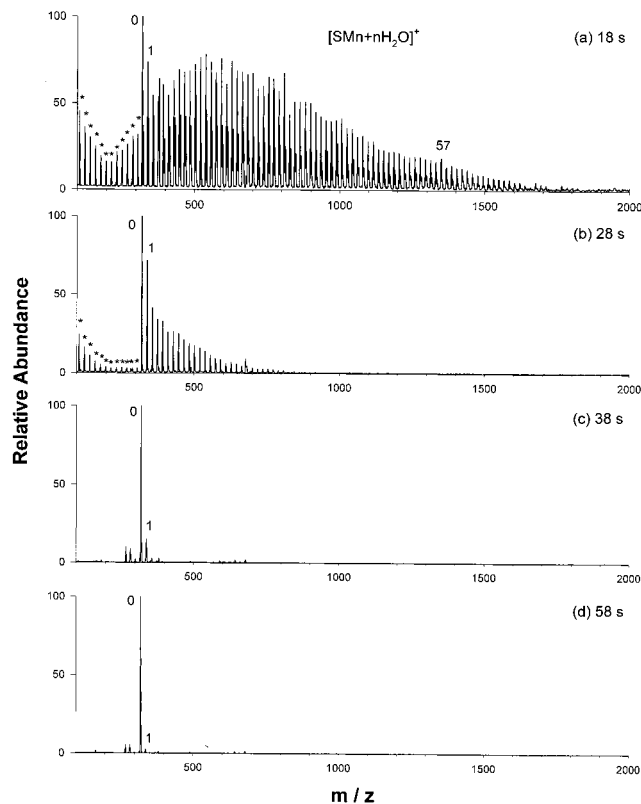


**Figure 2.** Water clusters of salen manganese complexes measured at various detection delays. No specific solvation is observed. Sample concentration is 50  $\mu\text{M}$  in 0.01% acetic acid solution. The asterisks indicate protonated water clusters.

**Table 1.** Rate Constants ( $\text{s}^{-1}$ ) for the Evaporation Reactions of Dihydrates of Salen Transition-Metal Complexes

	$[\text{SCr} + 2\text{H}_2\text{O}]^+$	$[\text{SMn} + 2\text{H}_2\text{O}]^+$	$[\text{SCo} + 2\text{H}_2\text{O}]^+$
$k_2^a$	$2.7 \times 10^{-2}$	$7.6 \times 10^{-1}$	$3.6 \times 10^{-1}$
$k_1^a$	$4.9 \times 10^{-2}$	$3.2 \times 10^{-1}$	$1.9 \times 10^{-1}$



**Evaporation Kinetics of Hydrated Salen Complexes.** As indicated in the mass spectra, water evaporation rates vary significantly for different metal ions. Table 1 compiles the rate constants for the dissociation reactions of the dihydrated salen complexes, obtained by the simulation method described in the Experimental Section. The rate constants for  $[\text{SCr} + n\text{H}_2\text{O}]^+$  are about an order smaller than those of  $[\text{SMn} + n\text{H}_2\text{O}]^+$  and  $[\text{SCo} + n\text{H}_2\text{O}]^+$  ( $n = 1$  and 2). Furthermore, the first loss of water from  $[\text{SCr} + 2\text{H}_2\text{O}]^+$  is two times slower than the second loss. Taking statistical factors into account where dihydrate complexes have two water molecules to lose while monohydrates have one, the first water loss is approximately four times slower than the second loss. Using the same argument, the first and second water loss processes occur at the similar rate for  $[\text{SMn} + 2\text{H}_2\text{O}]^+$  and  $[\text{SCo} + 2\text{H}_2\text{O}]^+$ . These observations are in qualitative agreement with water exchange rates of transition-metal aquo complexes, measured experimentally by isotopic labeling.<sup>18</sup> Water exchange rates are in the order of  $\text{Mn(III)} > \text{Co(III)} > \text{Cr(III)}$ , which matches the observed relative rates of water elimination for these metals in the present study.

**Evaporation Energetics of Hydrated Salen Complexes.** Water evaporation from the dihydrates of salen transition-metal

(17) Nelder, J. A.; Mead, R. *Comput. J.* **1965**, *7*, 308.

(18) Taube, H. *Chem. Rev.* **1952**, *50*, 69.

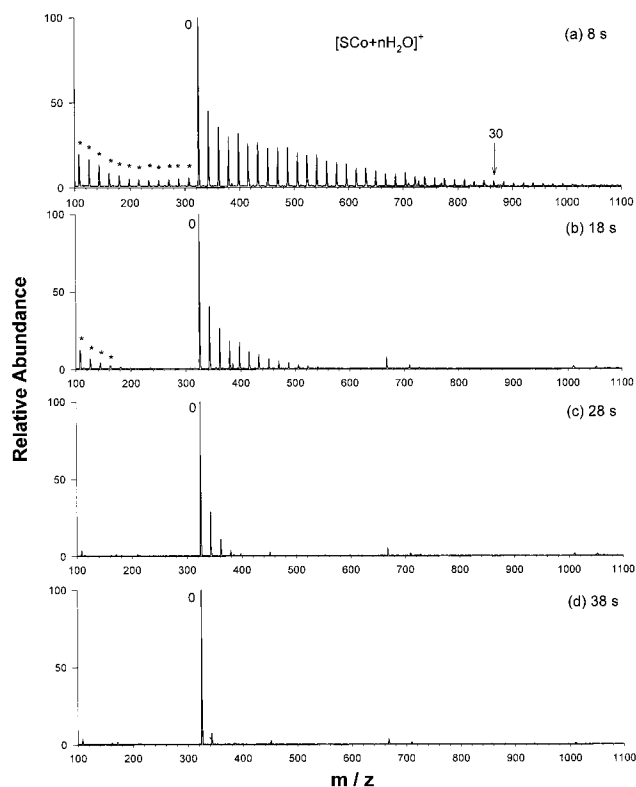


**Figure 3.** Water clusters of salen cobalt complexes measured at various detection delays. As with manganese complexes, the distribution exhibits no magic numbers. Sample concentration is  $80 \mu\text{M}$  in 0.01% acetic acid solution. The asterisks indicate protonated water clusters.

**Table 2.** Crystal Field Stabilization Energies (CFSEs) for the Salen Transition-Metal Complexes ( $M = \text{Cr}^{3+}$ ,  $\text{Mn}^{3+}$ ,  $\text{Co}^{3+}$ ) with Different Coordinations<sup>a</sup>

M	spin state	crystal field stabilization energy, Dq				
		$[\text{SM} + 2\text{H}_2\text{O}]^+$	$[\text{SM} + \text{H}_2\text{O}]^+$	$[\text{SM}]^+$	$\Delta_{21}$	$\Delta_{20}$
$\text{Cr}^{\text{III}}$		-12.00	-10.00	-14.56	2.00	-2.56
$\text{Mn}^{\text{III}}$	high	-6.00	-9.14	-12.28	-3.14	-6.28
	low	-16.00	-14.57	-19.70	1.43	-3.70
$\text{Co}^{\text{III}}$	high	-4.00	-4.57	-5.14	-0.57	-1.14
	intermed.	-14.00	-18.28	-22.56	-4.28	-8.56
	low	-24.00	-20.00	-29.12	4.00	-5.12

<sup>a</sup>  $\Delta_{21}$  and  $\Delta_{20}$  are the difference in CFSEs for dihydrates and monohydrates and CFSEs for dihydrates and dehydrated complexes, respectively. The crystal field effects of the tetradentate ligand are hard to predict. One can approximate the crystal field effects by dividing it into four separate ligands, such as two trialkylamine and two phenoxide ions. However, even with the use of different Jørgensen's  $f$  constants, the resultant energetics for the dissociation reactions do not change much.

complexes leads to changes in crystal field stabilization energies due to the varied coordination of the central metal ions. With two water molecules attached, the complex forms an octahedral complex, while  $[\text{SM} + \text{H}_2\text{O}]^+$  and  $[\text{SM}]^+$  form square pyramidal and square planar complexes, respectively. Assuming the same crystal field effects (the same Jørgensen's  $f$  constant) for all six coordinating sites (two nitrogens and two oxygens from the tetradentate ligand and two waters), the estimated crystal field stabilization energies (CFSEs) for the different salen transition-metal complexes are given in Table 2. On the basis of the CFSEs, one can construct an energy level diagram as shown in Figure 5. Figure 5 compares the changes in CFSEs with water evaporation from  $[\text{SCr} + 2\text{H}_2\text{O}]^+$  (Figure 5a) and  $[\text{SMn} + 2\text{H}_2\text{O}]^+$  (Figure 5b). Taking only d-orbital energies into account, the first loss of water from  $[\text{SCr} + 2\text{H}_2\text{O}]^+$  is calculated to be

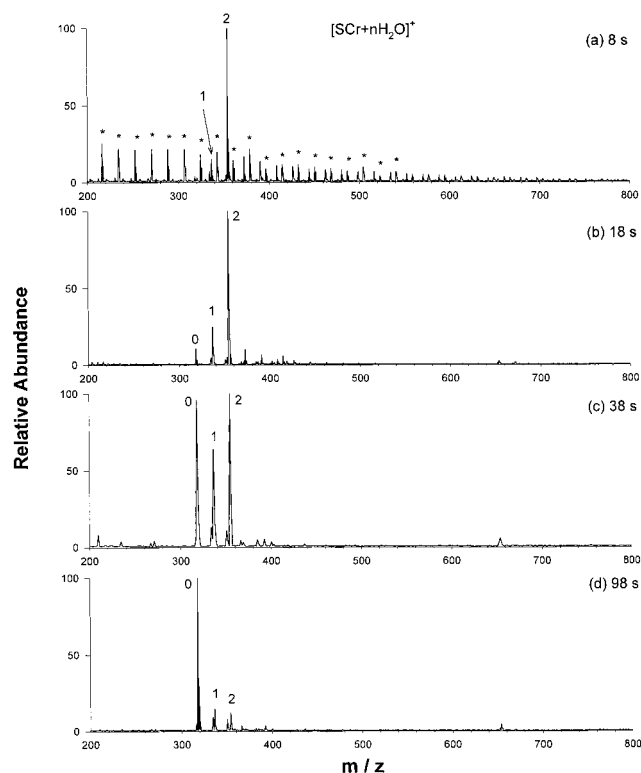


**Figure 4.** Water clusters of salen chromium complexes measured at various detection delays. The mass spectra clearly indicate that the dihydrate has special stability. Sample concentration is  $80 \mu\text{M}$  in 0.01% acetic acid solution. The asterisks indicate protonated water clusters.

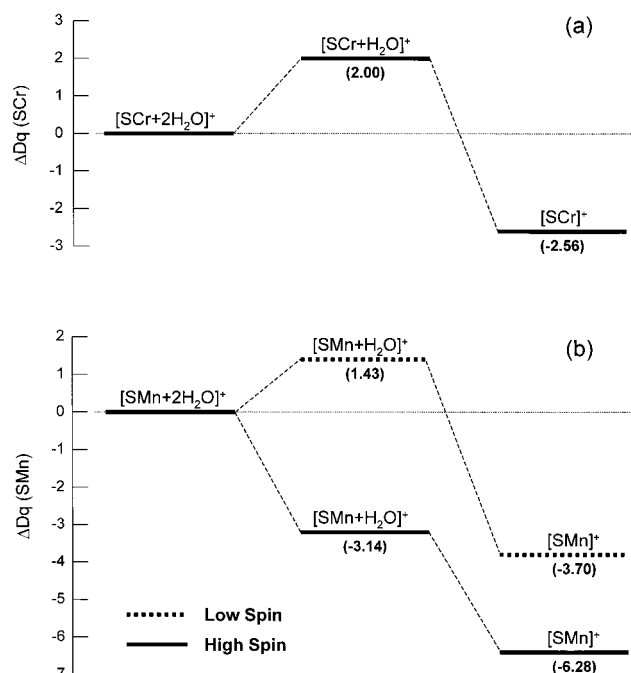


**Figure 5.** Changes in crystal field stabilization energies with water evaporation from  $[\text{SCr} + 2\text{H}_2\text{O}]^+$  (a) and  $[\text{SMn} + 2\text{H}_2\text{O}]^+$  (b). Evaporation kinetics observed in the present study indicates a high-spin state for  $[\text{SMn} + 2\text{H}_2\text{O}]^+$ .

an endothermic process while the second loss of water is exothermic. This accounts for the fact that the first dissociation reaction is four times slower in rate than the second. For the case of  $[\text{SMn} + 2\text{H}_2\text{O}]^+$ , we have two possible energetics for the dissociation reaction, corresponding to high- and low-spin complexes. For a low-spin complex, the energetics of the

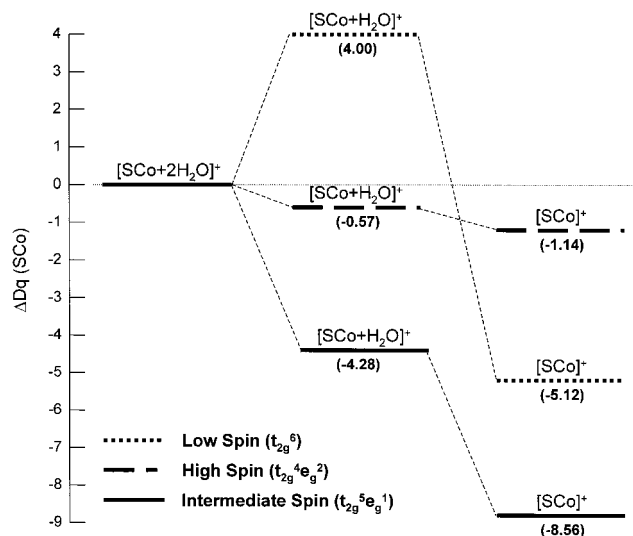


**Figure 6.** Changes in crystal field stabilization energies with water evaporation from  $[\text{SCo} + 2\text{H}_2\text{O}]^+$  for different spin states.

reaction is similar to that of  $[\text{SCr} + 2\text{H}_2\text{O}]^+$  and the dihydrate peak would be a strong peak. However, for a high-spin complex, the two losses of water from  $[\text{SMn} + 2\text{H}_2\text{O}]^+$  are both exothermic with the same energy increments. The kinetics observed in the present study is consistent with a high-spin salen manganese complex. The room-temperature magnetic moments of  $[\text{SMn} + 2\text{H}_2\text{O}]\text{ClO}_4 \cdot n\text{H}_2\text{O}$  are measured to be in the range of 4.7–5.0  $\mu_B$ , close to the spin-only value of 4.9  $\mu_B$  expected for a magnetically dilute high-spin  $d^4$  manganese(III) ion.<sup>19</sup>

Figure 6 shows the energetics for the dissociation reaction of  $[\text{SCo} + 2\text{H}_2\text{O}]^+$  with low ( $^1A_{1g}(t_{2g}^6)$ ), intermediate ( $^3T_{1g}(t_{2g}^5(e_g)^1)$ ), and high ( $^5T_{2g}(t_{2g}^4(e_g)^2)$ ) spin state as different possibilities. The evaporation kinetics indicates a high-spin or intermediate spin state for the salen cobalt complex. However, the magnetic susceptibility measured for  $[\text{SCo} + 2\text{H}_2\text{O}]\text{I} \cdot n\text{H}_2\text{O}$  is very low, suggesting a diamagnetic low-spin complex. Contrary to general expectations, it was observed that in solution the low-spin cobalt(III) aquo ion,  $\text{Co}(\text{H}_2\text{O})_6^{3+}$ , exchanges coordinated water with water molecules at high rates.<sup>20</sup> It was then suggested that the labile high-spin state ( $^5T_{2g}$ ) of  $\text{Co}(\text{H}_2\text{O})_6^{3+}$  might be within 4 kcal/mol of the ground state and thus accessible thermally. This postulate subsequently was supported by Gray and co-workers, who calculated the energy gap between  $^1A_{1g}$  and  $^5T_{2g}$  to be about 4 kcal/mol with an energy barrier of 5.4 kcal/mol associated with the curve crossing.<sup>21</sup> They pointed out that the potential energy curve for the  $^5T_{2g}$  state is displaced relative to the potential curve of the ground state due to Jahn–Teller distortion of the excited state<sup>22</sup> (Figure 7) and concluded that the quintet state plays a role in the lability of the aquo ion. The same should apply for the dissociation reaction of  $[\text{SCo} + 2\text{H}_2\text{O}]^+$ . As the water dissociates from the complex (increasing  $Q$  in Figure 7), the complex undergoes curve

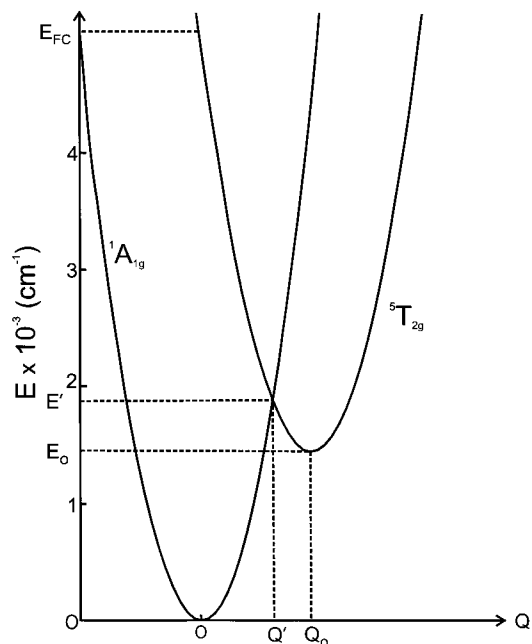


**Figure 7.** Potential energy curves for the  $^1A_{1g}$  and  $^5T_{2g}$  states for  $\text{Co}(\text{H}_2\text{O})_6^{3+}$ .  $Q$  is the distance between cobalt(III) and the water ligand. Taken from ref 21.

crossing to the  $^5T_{2g}$  state followed by dissociation. When the complex is in a high-spin state, the two evaporation processes are exothermic as shown in Figure 6, which is consistent with our observation that the complexes are labile (Figure 3).

## Conclusions

Water evaporation from extensively hydrated salen transition-metal complexes formed by operation of an electrospray ion source in a “soft sampling” mode has been studied. The generation of hydrated organometallic compounds such as salen transition-metal complexes in the gas phase provides a unique possibility for studying metal ligand interactions in a counterion free environment. The evaporation kinetics are observed to be heavily dependent on the central metal ion, in accordance with ligand field theory predictions for d-orbital energy changes resulting from elimination of water. The lability of the salen cobalt dihydrate complex indicates that the labile high-spin state is likely to be involved in the dissociation reaction. These studies can readily be extended to consider a range of ligands in addition to water, and the experimental methodology can be applied to study other important organometallic compounds such as porphyrins. Examination of the temperature dependence of the water loss rates is also of fundamental interest. Experiments to address this issue are underway in our laboratory.

**Acknowledgment.** The authors are grateful to Professor Harry B. Gray for helpful discussions and Mr. Joshua Maurer for acquiring SQUID data. This work was supported in part by the National Science Foundation under Grant CHE-9727566. Funds for instrument development have been provided by ARPA and the DOD-URI program (ONR-N0014-92-J-1901). We are also indebted to the Beckman Foundation and Institute for the initial funding and continuing support of the research facilities.

(19) Bermejo, M. R.; Castineira, A.; Garcia-Monteagudo, J. C.; Rey, M.; Sousa, A.; Watkinson, M.; McAuliffe, C. A.; Pritchard, R. G.; Beddoes, R. L. *J. Chem. Soc., Dalton Trans.* **1996**, 2935.

(20) Friedman, H. L.; Hunt, J. P.; Plane, R. A.; Taube, H. *J. Am. Chem. Soc.* **1951**, 73, 4028.

(21) Winkler, J. R.; Rice, S. F.; Gray, H. B. *Comments Inorg. Chem.* **1981**, 1, 47.

(22) Wilson, R. B.; Solomon, E. I. *J. Am. Chem. Soc.* **1980**, 102, 4085.